https://doi.org/10.5194/egusphere-2024-3191
Preprint. Discussion started: 5 December 2024

Low-temperature thermochronology and its geological significance in the central and northern section of the western margin of the Ordos Basin

Guangyuan Xing [1, 2], Zhanli Ren[1, 2*], Kai Qi [1, 2], Sasa Guo [1, 2], Yanzhao Liu [1, 2], Ying Zhang [3], Huaping Lan[4]

[1] *Department of Geology, Northwest University, Xi'an 710069, China;*

[2] *State Key Laboratory of Continental Dynamics, Northwest University, Xi'an 710069, China;*

[3] *Reseach Institute of Yanchang Petroleum(Group) Co.Ltd., Xi'an 710075, China;*

[4] *Research Institute No. 203 of Nuclear Industry, Xi'an 710000, China*

Correspondence to: Zhanli Ren

E-mail: renzhanl@nwu.edu.cn

Abstract: The study of low-temperature thermochronology at plate edges provides favorable constraints for regional tectonic evolution and surface processes. Based on the existing thermochronological data of multiple cooling events since the Mesozoic era, we conducted apatite fission track and apatite (U-Th)/He studies on drilling samples from the middle and northern parts of the western margin of the Ordos Basin, revealing the uplift and cooling history and differences in the middle and northern parts of the western margin of the Ordos Basin. The new thermal history simulation results show that the Zhuozishan Mountain(Mt.) part experienced large-scale uplift in the Late Jurassic (160Ma-150Ma), slow uplift at 130Ma-30Ma, and severe uplift after 30Ma; The Taole - Hengshanbao part began to uplift at 155Ma-145Ma, slowly uplifted at 145Ma-30Ma, and then violently uplifted; The Majiatan - Huianbao part experienced large-scale uplift at 158Ma-137Ma, with a slightly slower

https://doi.org/10.5194/egusphere-2024-3191
Preprint. Discussion started: 5 December 2024

uplift rate at 137Ma-110Ma, and entered a severe uplift stage again at 70Ma-50Ma. The Late Jurassic tectonic uplift indicated by thermochronology corresponds to the formation of the western margin thrust fold structure, with the northern and southern sections starting earlier and the middle section starting slightly later. This is related to the different tectonic evolution and stress in their location, and the differences in uplift rate and time may be related to the impact of multiple Yanshanian orogeny on the region.

Keyword： Ordos Basin；North China Block；Plate convergence；Low-temperature thermochronology；Yanshanian orogeny

1 Introduction

The North China Craton, as one of the oldest cratons in the world, has a long history spanning 3.8 billion years (Zhai, 2010; Zhang et al., 2018). Having undergone prolonged and complex tectonic evolution, it records nearly all major tectonic events from ancient to the present, especially preserving multi-phase evolutionary remnants since 1.8 billion years ago (Peng et al., 2022). The Ordos Block is part of the North China Craton and one of its core geological units (Bao et al., 2019; Zhai, 2021). The present-day Ordos Basin, in a narrow sense, is located in the western part of the North China Craton. It was formed on the foundation of the North China Craton through multiple phases of transformation,

https://doi.org/10.5194/egusphere-2024-3191
Preprint. Discussion started: 5 December 2024

particularly since the Mesozoic, eventually developing into a residual intracratonic basin (Ren et al., 1995; Zhai, 2021). This basin is superimposed on a large Paleozoic basin, making it a composite basin (Liu et al., 2005). The Ordos Basin contains the most complete sedimentary strata in the North China region and is rich in multiple energy resources, including oil, gas, coal, and uranium, making it a highly resource-abundant basin.

The thrust belt along the western margin of the Ordos Basin spans across different tectonic units, including the North China Craton, the Alxa Block, the Central Asian Orogenic Belt, the Qinling Orogenic Belt, and the northeastern edge of the Tibetan Plateau (Fig.1). It is one of the regions with the most intense tectonic deformation within the Chinese mainland since the Mesozoic, recording numerous intracontinental deformation and orogenic events since the Phanerozoic. Additionally, the western margin of the Ordos Basin lies in the northern segment of the North-South Tectonic Belt of China, connecting different tectonic units between the western and eastern parts of northern China (Dong et al., 2021).

The study area is located in the central-northern section of the western margin of the Ordos Basin (Fig. 1). Influenced by multiple tectonic movements, the region has a complex evolutionary history, with several large-scale, north-south-oriented thrust faults. In general, the

https://doi.org/10.5194/egusphere-2024-3191
Preprint. Discussion started: 5 December 2024

northern part of this tectonic belt is believed to result from interactions between adjacent tectonic blocks. Over the years, various scholars have conducted extensive research on the structural characteristics and properties of the northern section of the western margin (Yang et al., 1986; Tang et al., 1988, 1992; Gan et al., 1990; Liu et al., 1995; Zhao et al., 1990), its formation mechanisms (Liu et al., 1997; Liu et al., 2005; Ouyang et al., 2012; Yang et al., 2011; Yang et al., 2006, 2008; Zhao et al., 2003, 2006, 2007a, c), and provenance (Jiang et al., 2019). Regarding the overall uplift process along the western margin, many scholars, using apatite fission track methods, suggest that the uplift in the southern section of the western margin began in the Middle to Late Jurassic (Chen et al., 1999, 2007; Gao et al., 2000; Zhang et al., 2000; Zhao et al., 2003, 2006, 2007b; Zhao et al., 2017; Li et al., 2019; Ma et al., 2019; Peng Heng, 2020; Tian et al., 2023). Due to the presence of an east-west transfer zone in the Qingtongxia-Majiatan area, the western margin can be divided into three distinct tectonic systems: southern, central, and northern, based on differences in structural characteristics and sedimentation (Zhao et al., 2006). In the northern part of the western margin, including the Helanshan Mt. region, low-temperature thermochronology studies are relatively scarce and have mainly focused on the Helanshan Mt. area (Ma et al., 2019; Zhao et al., 2007a; Liu, 2010), the Zhuozishan Mt. region (Zhuo, 2015; Li, 2006), the 38°N Tectonic

https://doi.org/10.5194/egusphere-2024-3191
Preprint. Discussion started: 5 December 2024

Belt and adjacent areas (Gao, 2014; Zhao et al., 2007b, c; Ma et al., 2019; Li, 2019), and drilling wells such as LS1 well, T1 well, and TS1 well(Ren et al., 1995).

From the limited published thermochronological data, it is evident that the study area entered an uplift evolution stage during the Mesozoic, but the timing and rate of uplift vary across different regions. The structural differences between the basin margin and the interior have not been well clarified. Current research lacks a comprehensive perspective and does not provide a systematic understanding of tectonic events in the central-northern section of the western margin of the Ordos Basin since the Mesozoic. This greatly limits further insights into the overall tectonic evolution of the area and poses significant challenges for deeper research into intracontinental deformation in the basin and its surrounding regions.

This study utilizes low-temperature thermochronology methods, combined with thermal history modeling and existing geological evidence, to precisely constrain the uplift and cooling history of the central-northern section of the western margin of the Ordos Basin. The research helps improve our understanding of the evolution and tectonic processes in this region since the Mesozoic, providing important evidence for studying the formation and evolution of the Ordos Basin and the tectonic deformation that occurred along the basin's margins during the Mesozoic. Additionally, it offers a foundational reference for future oil and gas exploration efforts

https://doi.org/10.5194/egusphere-2024-3191
Preprint. Discussion started: 5 December 2024

in the western margin of the basin.

2 Geological setting

The Ordos Basin, as one of the key geological units of the North China Craton, is a large composite basin formed during different periods, across varying extents, and under diverse geodynamic settings (Ren et al., 2020). Based on the basin types and tectonic evolutionary characteristics of different eras, the basin’s evolution can be divided into several stages: Archean-Paleoproterozoic basement formation stage, Mesoproterozoic - Neoproterozoic rift basin development stage, Early Paleozoic stable continental margin sedimentation stage, Late Paleozoic to Middle Triassic intracratonic basin evolution stage, Late Triassic to Jurassic intracontinental depression basin evolution stage, Early Cretaceous westward contraction of the depression basin, Late Cretaceous to Cenozoic significant uplift, Formation of Cenozoic fault-depression basins in the surrounding areas (Liu et al., 2006; Ren et al., 2020;Li, 2006).

In order to more precisely define the differences in the later uplift and cooling processes, this article further divides the research area into the Zhuozishan Mt. part, the Taole-Hengshanbao part, and the Majiatan-Huianbao part.

https://doi.org/10.5194/egusphere-2024-3191
Preprint. Discussion started: 5 December 2024

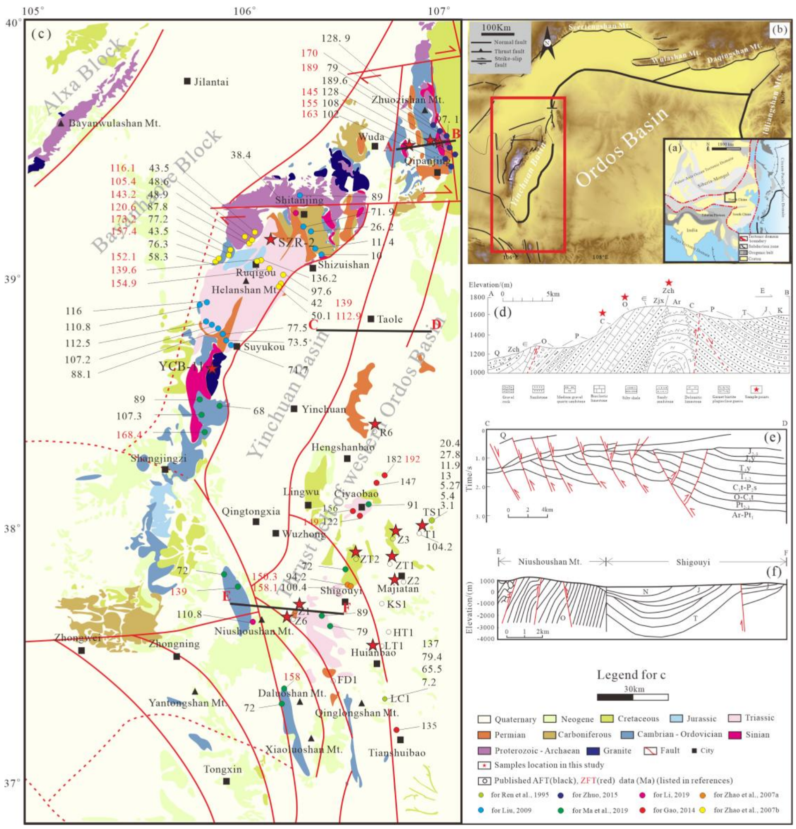

Fig.1 (a) Tectonic setting of China (modified from Peng et al., 2019), (b) Digital elevation model of the Ordos basin (modified from Shi et al., 2020), (c) Geological map of the central-northern section of the western margin of the Ordos Basin (modified from Ma, 2019) and compilation of previously published low-temperature thermochronology data, (d) W - E trending simplified geological profile A-B studied in this article (modified from Zhuo， 2015), (e) W - E trending simplified geological profile C-D studied in this article (modified from Zhao， 2006), (f) W - E trending simplified geological profile C-D studied in this article (modified from Ma, 2019).

In the Zhuozishan Mt. part, faults thrust from west to east, consisting of the Bayin’aobao thrust sheet, the Wuhushan thrust sheet, the Gandel Mountain thrust sheet, and the Zhuozishan Mt. thrust sheet. The Zhuozishan anticline is located near the basin, with an east-west length of approximately 10 km. The core of the anticline exposes older strata, with Archean granitic gneiss of the Qianlishan Group at its core. Moving

https://doi.org/10.5194/egusphere-2024-3191
Preprint. Discussion started: 5 December 2024

westward, it sequentially exposes the Changcheng System Huangqikou Formation, Jixian System Wangquankou Formation, Cambrian Taosigou Formation, Hulusitai Formation, Zhangxia Formation, Abuqiehai Formation, Ordovician Sandaokan Formation, Zhuozishan Formation, and the Permian Shanxi Formation and Shihezi Formation (Fig. 1d).

In this study, the central part of the research area is defined as the Taole-Hengshanbao part. Overall, the structural line in this region is distributed in a nearly north-south orientation, and its structural characteristics differ from those of the Zhuozishan Mt. part. The faults in this area exhibit high-angle thrusting from east to west, characterized by a series of imbricated thrust faults (Fig. 1e). Additionally, this part corresponds to the Yinchuan Graben to the west, and their tectonic evolution is closely related (Zhao, 2006).

The Majiatan-Huianbao part is characterized by typical thrust nappe structures, with four west-dipping thrust faults developing from west to east. These faults exhibit steep upper angles and gentle lower angles. From west to east, the major thrust sheets include the Weizhou thrust sheet, Qinglongshan thrust sheet, Shigouyi thrust sheet, and Yandunshan thrust sheet. Among them, the Shigouyi thrust sheet, in an anticlinal form, is situated between the Qingshanlong Fault and the Huianpu-Shajingzi Fault (Fig. 1f).

In the Hengshanbao area, east-dipping faults are dominant, while the

https://doi.org/10.5194/egusphere-2024-3191
Preprint. Discussion started: 5 December 2024

Majiatan-Huianbao part primarily features large west-dipping faults. The 38°N structural zone between these regions plays a regulatory role, and the different structural styles on both sides have created distinct types of traps. This has resulted in the concentration of oil and gas fields along the western margin of the basin, particularly in the Shigouyi and Majiatan areas (Gao, 2014; He et al., 2021).

3 Sampling strategy and methodology

3.1 Previous thermochronological data

This study collected a total of 85 published low-temperature thermochronology data from the western margin of the Ordos Basin, specifically between the Zhuozishan Mt. and the Tianshuibao, including 62 apatite fission track ages and 23 zircon fission track ages (Fig. 2). Samples with higher mineral closure temperatures exhibit older apparent ages. The ages of apatite samples range from 3.1 Ma to 189.6 Ma, while zircon fission track ages range from 105.4 Ma to 192 Ma. These findings indicate a long cooling history and a complex uplift process in the study area. Based on the collected data, we plotted histograms and kernel density estimation curves, revealing that the density peaks for apatite fission tracks and zircon fission tracks are at 78 Ma, 101 Ma, and 153 Ma, respectively.

https://doi.org/10.5194/egusphere-2024-3191
Preprint. Discussion started: 5 December 2024

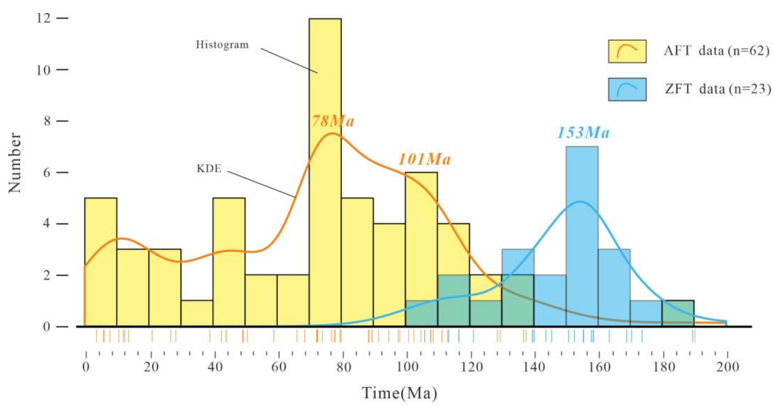

Fig.2 Histogram and kernel density estimation (KDE) plot of published geochronological dates in the central-northern section of the western margin of the Ordos Basin. The bandwidth and bin width are both set to 10 Ma for all plots when the graph is drawn.

In summary, previous thermochronological data indicate that multiple cooling events have occurred in the region since the Mesozoic era (Ren et al., 1995; Zhao et al., 2007a, b; Liu, 2010; Zhuo, 2015; Gao, 2014; Li, 2019; Ma et al., 2019). However, due to a lack of chronological methods, the cooling history of the study area during the late Cenozoic has not been well constrained.

3.2 Sample collection and experimental methods

This study applies thermochronology to constrain the spatiotemporal evolution of the upper few kilometers of the lithosphere. As one of the most widely used and effective thermochronological methods (Gleadow and Seiler, 2015; Peng, 2020), apatite fission track analysis is sensitive to temperature variations in the range of 60°C to 120°C (the partial annealing zone), while apatite (U-Th)/He dating is suitable for defining the time-temperature history in the range of 40°C to 75°C (Ketcham,

https://doi.org/10.5194/egusphere-2024-3191
Preprint. Discussion started: 5 December 2024

2005; Gallagher, 2012; Flowers et al., 2015; Farley et al., 2002).

To systematically study the differences in uplift and cooling in the central-northern part of the western margin, the relationship between structural evolution at the basin edge and within the basin, and to address the current gaps in thermochronology in the research area, this study collected 16 valuable samples, including 11 core samples from 9 drilling wells and 5 field outcrop samples. Apatite fission track analysis and apatite (U-Th)/He dating were employed for chronological analysis. The samples are well-distributed across the entire central-northern region of the western margin and are representative of various stratigraphic levels. After obtaining the samples, apatite was separated using conventional heavy liquid and magnetic separation methods.

All 16 samples were analyzed using apatite fission track (AFT) methodology. After selecting mineral grains, the samples were prepared, tested, and analyzed at the Petroleum Thermochronology Laboratory in the Department of Geology at Northwest University. The calculation method for AFT ages follows Hasebe et al. (2004), and ages were analyzed using RadialPlotter software (Vermeesch, 2009) (Fig.3, 4a). Additionally, the HeFTy software was utilized to simulate the cooling history (Ketcham, 2005).

https://doi.org/10.5194/egusphere-2024-3191
Preprint. Discussion started: 5 December 2024

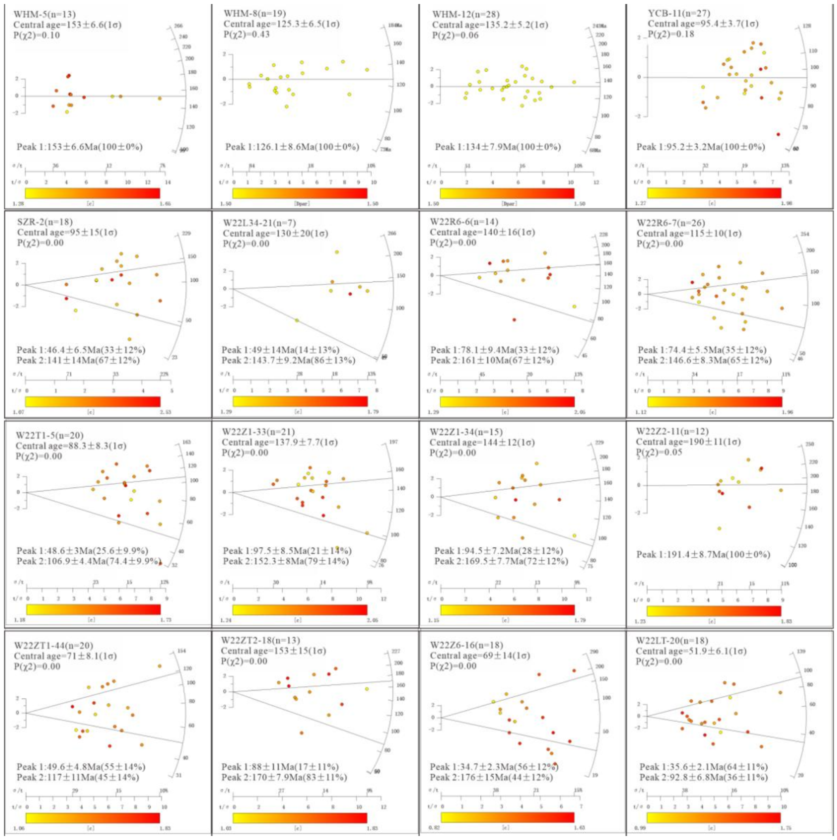

Fig.3 AFT age Radial plots for samples (WHM-5, 8, and 12 are the data that the author will soon publish, while the rest are newly published data in this paper).

Additionally, following three criteria—selecting well-formed, pure grains and ensuring that the crystal dimensions perpendicular to the c-axis exceed 60-70 μm—apatite grains from samples Z1-33 and ZT2-18 were chosen under a high magnification (160x) binocular microscope for (U-Th)/He (AHe) dating. This experiment was conducted at the Argon-Argon and U-Th-He Geochronology Laboratory of the Institute of Geology and Geophysics, Chinese Academy of Sciences. The thermal history of the samples was also modeled using HeFTy software (Ketcham, 2005).

https://doi.org/10.5194/egusphere-2024-3191
Preprint. Discussion started: 5 December 2024

4 Results

4.1 Low-temperature thermochronology results

4.1.1 Zhuozishan Mt. part

The AFT central ages of the three sandstone samples from the Zhuozishan Mt. part (WHM-5, WHM-8, WHM-12) are 153±6.6 Ma, 125±6 Ma, and 135±5 Ma, respectively, all of which are significantly younger than the stratigraphic ages from which the samples were derived. The average track lengths are 12.16±1.54 μm, 11.43±1.55 μm, and 13.3±1.7 μm, all of which are shorter than the spontaneous track original length of 16.3±0.9 μm, indicating that the samples have undergone annealing and cooling processes. All three samples passed the χ^2 test ($P(\chi^2) > 5\%$), suggesting that each sample contains a single age component. The RadialPlotter software provided single ages of 153±6.6 Ma, 126.1±8.6 Ma, and 134.7±7.9 Ma (Fig. 4b), which are consistent with the central ages within a certain error range. The age of 153±6.6 Ma may represents a tectonic event in the Late Jurassic, while 134.7±7.9 Ma may corresponds to an early tectonic event in the Early Cretaceous, and 126.1±8.6 Ma may indicates a tectonic event in the Late Early Cretaceous.

4.1.2 Taole-Hengshanbao part

The AFT central ages of the two samples from well R6 (R6-6 and R6-7) are 140.4±15.7 Ma and 115.3±10.2 Ma, with average track lengths

https://doi.org/10.5194/egusphere-2024-3191
Preprint. Discussion started: 5 December 2024

of 11.66±1.02 μm and 12.1±1.52 μm, respectively. The AFT central age of the sample from well L34 (L34-21) is 130±19.8 Ma. In the Helanshan Mt. area, the AFT central ages of samples SZR-2 and YCB-11 are 95.2±14.8 Ma and 95.4±3.7 Ma, with average track lengths of 12.01±1.68 μm and 12.88±1.11 μm, respectively. The AFT central ages of these five samples in this region are significantly younger than the stratigraphic ages from which they were derived, indicating that the samples have undergone annealing and cooling processes. Only the YCB-11 sample passed the χ^2 test, with the RadialPlotter software providing a single peak age of 95.2±3.2 Ma. The remaining four samples did not pass the χ^2 test, suggesting that each sample contains at least two age populations. The RadialPlotter software (Vermeesch, 2009) was used to decompose the ages, and these peak ages record potential tectonic activities in this region during the Late Jurassic, early Early Cretaceous, late Early Cretaceous, Late Cretaceous, and Eocene epochs (Fig. 4c).

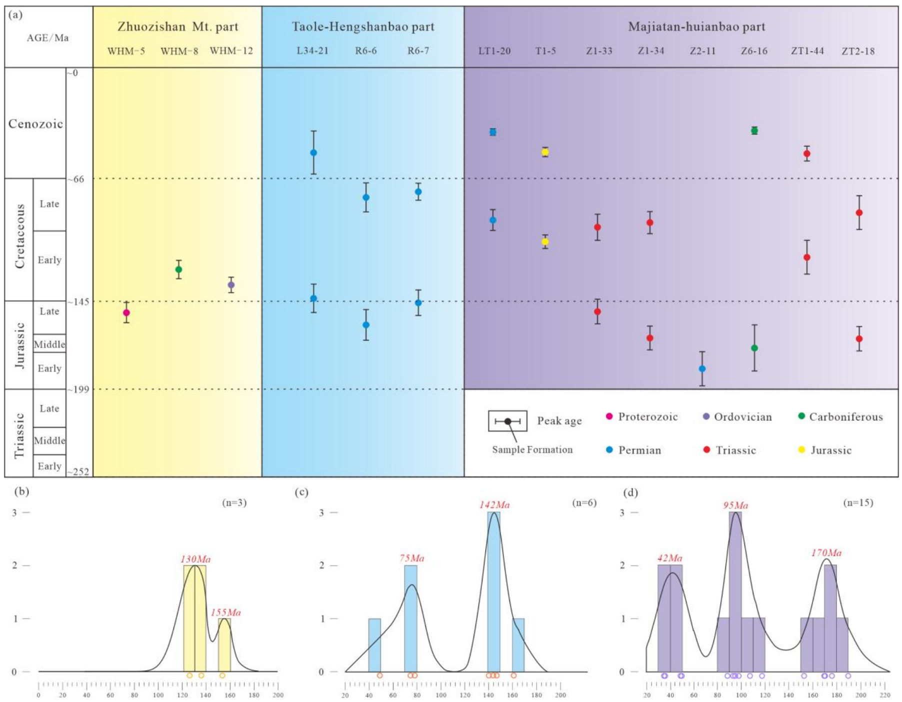

Fig.4 (a) The peak age distribution map of the three areas in the study region. (b), (c), (d), Histogram and kernel density estimation (KDE) plot of new geochronological dates in Zhuozishan Mt. part, Taole-Hengshanbao part, and Majiatan-Huianbao part.

4.1.3 Majiatan-Huianbao part

Due to this region being a sweet spot for oil and gas exploration, a large number of drilling samples are available. Except for sample Z2-11, which passed the χ^2 test, the remaining samples did not pass the test. The ages range from 35.6 to 189.5 Ma and were statistically divided into three peak values: 42 Ma, 95 Ma, and 170 Ma. All of these ages are significantly younger than the stratigraphic ages from which they were derived, indicating that they have undergone uplift and cooling processes (Fig. 4d). The three single-grain AHe ages for sample Z1-33 range from 61.64 Ma to 67.06 Ma, while the three single-grain AHe ages for sample

https://doi.org/10.5194/egusphere-2024-3191
Preprint. Discussion started: 5 December 2024

ZT2-18 range from 50.69 Ma to 56.31 Ma, with no significant correlation to eU, recording late uplift and cooling events (Fig. 5).

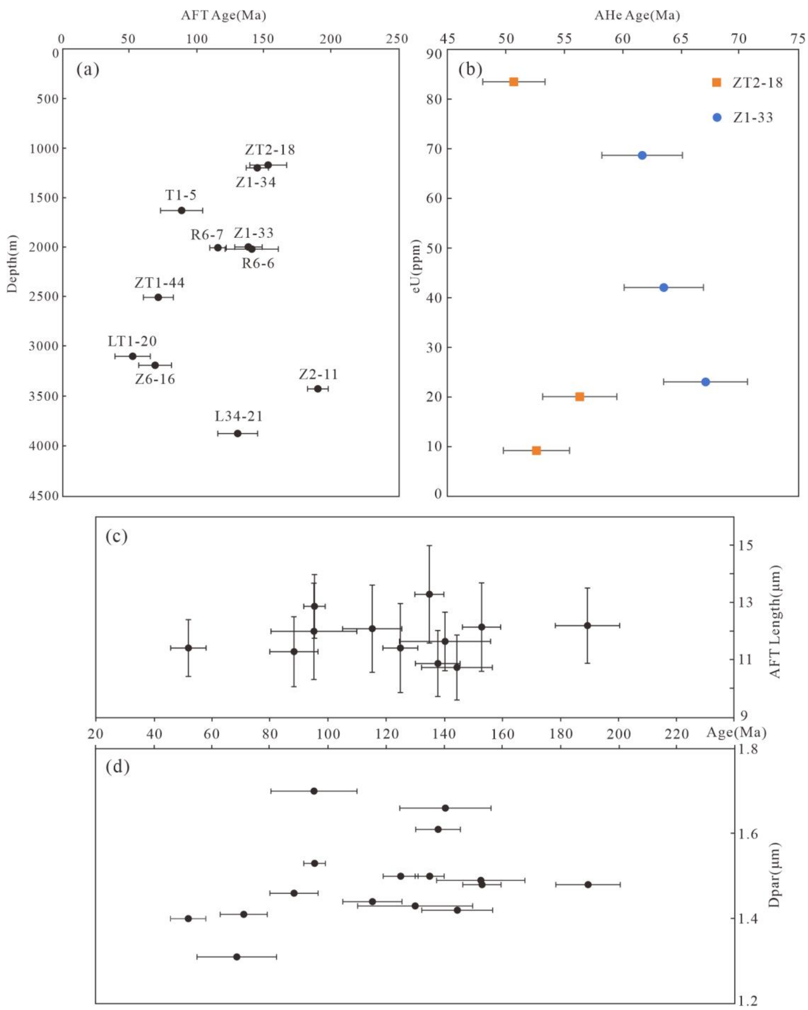

Fig.5 Relationships between AFT Age and (a) depth, (c) AFT length, and (d) Dpar, (b) relationships between AHe age and eU.

In addition, the correlation between track length and AFT age indicates a complex cooling history in the region. Considering the different annealing dynamics (Ketcham et al., 2007), the chemical composition of the grains may influence the AFT age and length (Carlson

https://doi.org/10.5194/egusphere-2024-3191
Preprint. Discussion started: 5 December 2024

et al., 1999; Barbarand et al., 2003). However, the Dpar values in the samples range from 1.31 μm to 1.70 μm, showing minimal variation and no significant correlation with the AFT ages. This suggests that the influence of chemical composition on AFT age is either minimal or nonexistent.

4.2. Thermal history modeling

Due to the complexity of annealing processes, the measured apparent ages lack any practical geological significance (Flowers et al., 2015). By utilizing the measured ages, track lengths, Dpar values, and other parameters, this thermal history can be inversely modeled (Ketcham, 2005). In this study, HeFTy version 1.6.7 was used for inverse modeling (Ketcham, 2005), in conjunction with all available low-temperature thermochronology data for path analysis. The Ketcham (2005) multi-dynamic annealing model was selected for the inversion simulation, along with the corrected confined track lengths. The original confined track length was set at 16.3 μm, and the present-day surface temperature was 20°C. The goodness-of-fit parameter (GOF) was used to indicate how well the simulation results matched the actual measurements; a higher value signifies a better fit. When the GOF value obtained from the simulation exceeds 0.05, it indicates that the simulation results are acceptable, while a GOF value greater than 0.5 indicates a very good match. The simulated ages and lengths both had GOF values greater than

https://doi.org/10.5194/egusphere-2024-3191
Preprint. Discussion started: 5 December 2024

0.5 and close to 1, suggesting that the simulation results closely aligned with the measured values.

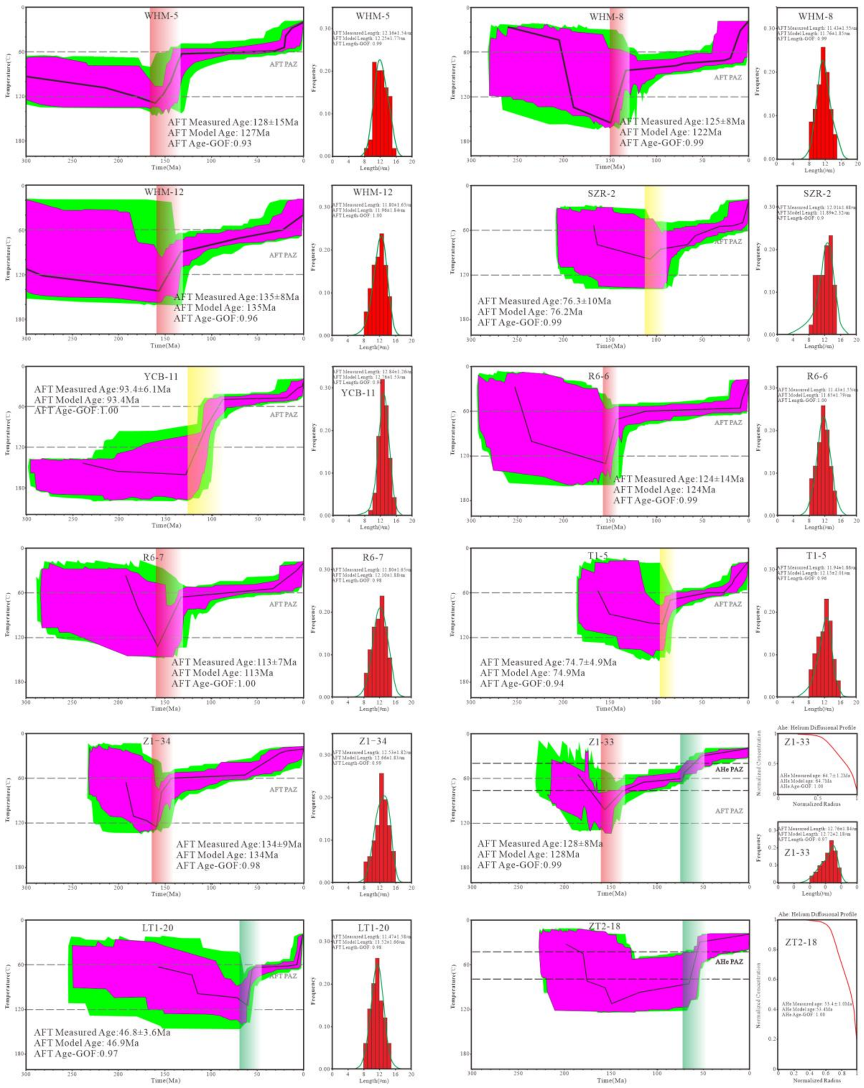

Fig.6 Thermal history inverse modeling calculated by HeFTy (Ketcham, 2005), using the model of Ketcham et al. (2007) and Flowers et al. (2009). HeFTy modeling tests possible t – T curves by using the Monte-Carlo inverse modeling approach. Shaded parts of different colors represent different cooling periods.

Among the 16 samples, 12 with more extensive length information were selected for thermal history simulation, representing a broad

https://doi.org/10.5194/egusphere-2024-3191
Preprint. Discussion started: 5 December 2024

distribution across the study area to assess their potential thermal history and determine their uplift cooling times. The goodness-of-fit parameters for both length and age in this simulation were above 0.90, indicating a good fit. The inverted time-temperature paths are shown in Fig. 6.

5 Discussion

From the thermal history simulation paths, the uplift initiation times for the three sample sections generally fall in the late Jurassic; however, there are still differences. The middle Taole-Hengshanbao part was uplifted later, while the northern and southern parts were uplifted earlier, which is related to the tectonic evolution and stress of their respective locations. Additionally, the uplift intensity varies from east to west across the regions. For example, in the northern part, the uplift rate of the Changcheng System, which is closer to the core of the syncline on the eastern side of the Zhuzishan syncline, is faster than that of the Paleozoic strata on the western side. The samples from the southern part indicate that uplift occurred earlier in the western samples compared to those in the eastern side. These observations are closely linked to the reverse thrusting and imbrication along the western margin (Fig. 7).

5.1 Uplift Process Differences and Geological Responses in the North-Central Western Margin Constrained by Low-Temperature Thermochronology

5.1.1 Zhuozishan Mt. part

https://doi.org/10.5194/egusphere-2024-3191
Preprint. Discussion started: 5 December 2024

The thermal history inversion results for the three samples from the northern Zhuozishan Mt. part indicate that the region underwent three major uplift stages after the Mesozoic: Late Jurassic (160 Ma - 150 Ma), This marks the first major uplift stage in the area, with an average uplift rate of ca. 45 m/Ma and an average cooling rate of ca. 2℃/Ma. This uplift corresponds to the early stages of the Yanshanian orogeny in the region, triggering reverse thrusting and imbrication, as evidenced by the inversion results of all three samples. Stratigraphically, the Late Jurassic deposits are largely absent in the study area, with the Middle Jurassic Anding Formation directly in contact with the Lower Cretaceous strata; Early Cretaceous (130 Ma - 30 Ma), This stage represents a period of slow cooling, suggesting the absence of significant tectonic events during this time. The timing and uplift differences among the samples during this phase may reflect the varying effects of different episodes of the Yanshanian orogeny (stages II, III, and IV) on the region; Cenozoic (since ca. 30 Ma), The most recent uplift stage is associated with the Himalayan orogeny, which caused further significant uplift in the region.

In terms of the spatial distribution of the Zhuzishan anticline (Fig. 1d), the WHM-5 sample from the Changcheng System on the eastern side of the anticline entered and exited the partial annealing zone earlier than the WHM-8 sample from the Taiyuan Formation on the western side. This sequence aligns with the recorded ages. Additionally, the eastern side,

https://doi.org/10.5194/egusphere-2024-3191
Preprint. Discussion started: 5 December 2024

closer to the core of the anticline, exhibits a faster uplift rate in the Changcheng System compared to the Paleozoic strata on the western side, with the Ordovician strata showing intermediate uplift rates. Combined with previous analyses of Mesozoic samples on the eastern flank of the Zhuzishan anticline, the general conclusion is that the core of the anticline experienced rapid uplift, while the flanks uplifted more slowly, indicating a differential uplift process (Zhuo, 2015).

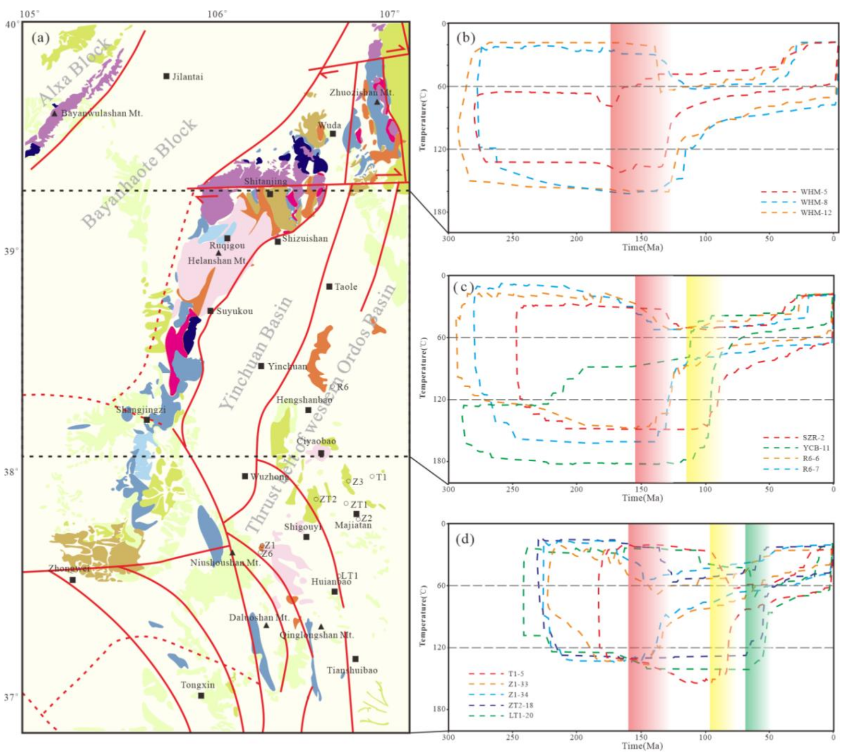

Fig.7 Summary of all available thermochronology modeling history (envelope path) for central-northern section of the western margin of the Ordos Basin.

5.1.2 Taole-Hengshanbao part

In the Taole-Hengshanbao part, two samples from well R6 have peak ages of 161 Ma, 146 Ma, 78 Ma, and 74 Ma, suggesting possible tectonic

https://doi.org/10.5194/egusphere-2024-3191
Preprint. Discussion started: 5 December 2024

events during the Late Jurassic and Late Cretaceous. The thermal history models of both samples show similar results, indicating three phases of uplift: Late Jurassic (155 Ma-145 Ma), a period of significant uplift begins; Early Cretaceous (145 Ma-30 Ma), this phase is characterized by slow uplift; Cenozoic (ca. 30 Ma-), a period of intense and rapid uplift occurs. The ages recorded in samples R6-6 and R6-7 are consistent within the error range. The slight differences in their AFT model results arise because R6-6 was located deeper, meaning it exited the partial annealing zone later than R6-7 during uplift. This caused the AFT age constraints for R6-6 to be slightly younger.

The uplift in this part is related to the uplift in the neighboring Helanshan Mountain region and the intense faulting and subsidence in the Yinchuan Graben. The thermal history models of the two Helanshan Mountain samples (SZR-2 and YCB-11) show a spatial pattern: the southern YCB-11 sample experienced rapid cooling at the end of the Early Cretaceous (130 Ma-95 Ma), followed by slow cooling until the Eocene (~35 Ma), after which it rapidly uplifted to the surface. The northern SZR-2 sample, however, shows a delayed cooling history, with cooling events occurring primarily after the Early Cretaceous. The uplift pattern, with earlier uplift in the south and later uplift in the north, aligns with previous studies on the Helanshan Mountain region (Ma et al., 2019).

https://doi.org/10.5194/egusphere-2024-3191
Preprint. Discussion started: 5 December 2024

5.1.2 Majiatan-Huianbao part

In the southern, Majiatan-Huianbao part, two samples from well Z1 (Z1-33 and Z1-34) indicate that uplift in the well began during the Late Jurassic (ca. 160 Ma). Combined AFT and AHe inversion results show that sample Z1-33 experienced rapid uplift between 158 Ma and 137 Ma, followed by slower uplift from 137 Ma to 110 Ma, and then entered another phase of intense uplift between 70 Ma and 50 Ma. Sample Z1-34, constrained only by AFT data, shows large-scale uplift starting from 160 Ma to 140 Ma, a slow uplift phase from 140 Ma to 64 Ma, and then a rapid uplift event. Since the temperature at 64 Ma is beyond the AFT-sensitive temperature range, the thermal history model of well Z1, especially for the later stages of uplift and cooling, is more reliably constrained by the dual-dating sample Z1-33. The AFT simulation of sample LT1-20 reveals an uplift event between 60 Ma and 55 Ma, and the AHe thermal history simulation of sample ZT2-18 similarly shows an uplift event from 62 Ma to 52 Ma. This indicates an early Cenozoic tectonic cooling event in the region. For the T1-5 sample, located in the Tianhuan syncline, uplift began at the end of the Early Cretaceous. This area previously had a complete sedimentary sequence and extensive sediment distribution, forming the thick Tianhuan syncline in the Ordos Basin (Zhao et al., 2007a).。

5.2 Transformation of the Meso-Cenozoic Tectonic Regime and

https://doi.org/10.5194/egusphere-2024-3191
Preprint. Discussion started: 5 December 2024

Regional Dynamic Background in the North-Central Western Margin

At the end of the Paleoproterozoic, the Ordos Block formed and merged with the North China Craton. Following this, under an extensional tectonic environment, large-scale rifting occurred, creating northeast-trending rift troughs with some structural inheritance from the basement. These troughs were subsequently covered by stratigraphic deposits from different periods (Bao et al., 2019; Zhao et al., 2019). In the Early Paleozoic, the Ordos region transitioned into a stable cratonic basin. During multiple marine transgressions and regressions, a set of widespread marine carbonate sediments, interbedded with clastic rocks, was deposited across the region. The large-scale Caledonian orogeny caused a depositional hiatus between the Ordovician and Carboniferous systems, resulting in an unconformable contact between the two. Since the Late Paleozoic, the Ordos Basin has transitioned from marine to terrestrial facies deposition, evolving from a coastal-continental margin to shallow marine sediments, dominated by swamp, deltaic, and fluvial deposits. During the Late Triassic to Early Cretaceous, the basin saw intracratonic fluvial-lacustrine sedimentation. Since the Late Cretaceous, the basin has experienced overall uplift and surrounding faulting. From the Late Mesozoic, the Ordos Basin became an independent sedimentary basin. Its sedimentary evolution has been primarily influenced by the

https://doi.org/10.5194/egusphere-2024-3191
Preprint. Discussion started: 5 December 2024

Mesozoic-Cenozoic tectonic systems, undergoing multiple sedimentary cycles and uplift-related transformations (Fig. 8).

The Yanshanian orogeny was the primary tectonic deformation period for the Ordos Basin, with the Late Jurassic tectonic movements being particularly intense. These movements caused the Jurassic and underlying sedimentary layers to become involved in widespread deformation, resulting in a clear angular unconformity with the overlying strata. This deformation was especially pronounced along the western margin of the basin, where much of the surface deformation that is observed today had already taken shape during this period (Darby et al., 2002). In the Early Cretaceous, the deep thermal material in the basin began to upwell, and the upper crust entered a tensional tectonic environment. Since the Late Cretaceous, the Ordos Basin has experienced significant uplift and erosion, a process that has continued to the present day (Ren et al., 2007, 2008, 2014, 2017, 2020, 2022).

https://doi.org/10.5194/egusphere-2024-3191
Preprint. Discussion started: 5 December 2024

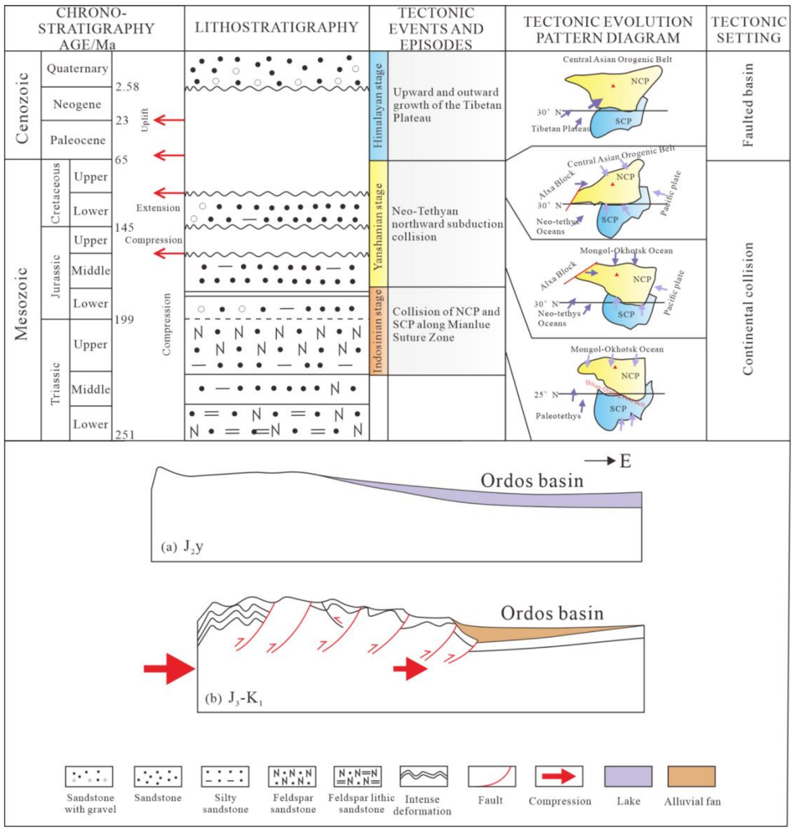

Fig.8 Dynamic model diagram of the northern part of the western margin of Ordos Basin.(Modified from Ma, 2019; Zhang et al., 2021; Peng et al., 2022)

During the Triassic period, the Indosinian Orogeny significantly impacted the region, leading to the final closure of the ancient Qinling-Qilian Ocean Basin. The continuous collision and compression of mountain ranges caused uplift and sedimentary hiatuses. As a result, the Late Triassic and Early Jurassic strata exhibit a parallel unconformity (Zhang et al., 2001).

In the Late Jurassic, the Yanshanian orogeny triggered the first major large-scale uplift in the study area. During this period, the compressional forces that were primarily north-south oriented during the earlier

https://doi.org/10.5194/egusphere-2024-3191
Preprint. Discussion started: 5 December 2024

Indosinian orogeny transitioned to an east-west orientation characteristic of the Yanshanian phase (Dong et al., 2007, 2008, 2015; Zhang et al., 2008). This tectonic uplift event aligns with the peak ages obtained from fission tracks at 170 Ma, 161 Ma, and 153 Ma. The tectonic evolution of this phase was controlled by several factors, notably the southwest Tethys tectonic domain, eastward compression from the Alxa Block , and the closure of the Okhotsk Ocean in the north during the Late Jurassic (Zhao et al., 2023). Additionally, far-field effects from the subduction of the Pacific Plate played a role (Darby et al., 2002, 2007; Faure et al., 2012; Liu et al., 1998; Yang et al., 2008; Zhang et al., 2020, 2021, 2022; Zhao et al., 2023). Previous paleomagnetic studies revealed that the Ordos Basin was undergoing a counterclockwise rotation during this period (Ma et al., 1993; Yang et al., 1999; Zhang et al., 2000). These regional tectonic processes collectively shaped the large-scale uplift and deformation seen during this period, marking a significant phase in the area's geological history. The comprehensive analysis of stress fields in the Late Jurassic indicates that multiple tectonic blocks around the Ordos Basin experienced subduction, collision, compression, and even mutual rotation. These interactions led to the folding and uplift of Jurassic strata, accompanied by a series of imbricate thrust faults pushing from west to east (Zhao et al., 1987; Ma et al., 2019; Zhang et al., 2021, 2022). In the northern section, the collision with the Alxa Block initiated significant

https://doi.org/10.5194/egusphere-2024-3191
Preprint. Discussion started: 5 December 2024

uplift, while in the southern part, the overall uplift of the Qilian Mountains and its thrusting into the basin resulted in strong thrusting structures. This contributed to the earlier onset of uplift in areas like Zhuozishan Mt. and the Majiatan-Huianbao regions. The compressional deformation shows a general pattern of stronger uplift and deformation in the west and at the margins, with weaker effects in the interior of the basin.

The Early Cretaceous was a crucial period in the evolution of the Ordos Basin. Northern China was under an extensional tectonic regime, linked to the broader lithospheric thinning and basin development of the North China Craton during the Early Cretaceous (Ren et al., 2020). In the central Taole region, extensional faults from this period are observable in seismic profiles (Zhao et al., 2007a). Towards the end of the Early Cretaceous, the regional tectonic stress field reversed due to the multiple phases of the Yanshanian orogeny (phases II, III, IV). The area was simultaneously influenced by the northward collision of the Yangtze Plate and the far-field effects of the Pacific Plate. The northern region was affected by the closure of the Okhotsk Ocean, and the western region continued to experience direct compression from the eastward movement of the Alxa Block (Yang et al., 2008; Zhang et al., 2020, 2022; Zhao et al., 2023). The previously deposited strata experienced intensified folding and uplift under compressional stress, resulting in significant structural

https://doi.org/10.5194/egusphere-2024-3191
Preprint. Discussion started: 5 December 2024

deformation. This led to the formation of large-scale south-north-oriented thrust faults and imbricate thrust structures. By this time, the region's major tectonic framework had largely formed, and subsequent tectonic movements primarily modified this existing structure.

During the Cenozoic, the tectonic deformation of the Ordos Basin was primarily driven by the collision between the Indian and Eurasian plates, with significant tectonic activity occurring during the Eocene to Miocene. The continued Himalayan orogeny caused strong tectonic movements in the region, leading to further uplift of the mountains, with the strata predominantly displaying parallel and angular unconformities. This tectonic activity has significantly shaped the present-day landscape. The neighboring Alxa region, located at the northeastern edge of the Tibetan Plateau, was affected by the plateau's Cenozoic uplift. Its deformation is closely linked to the evolution of the Tibetan Plateau (Zhang et al., 2023; Rao et al., 2016; Lei et al., 2022). Concurrently, the Pacific Plate continued its northwestward subduction during this period. Numerous geochronological records document the uplift and northeastward expansion of the northeastern Tibetan Plateau during the Cenozoic, particularly in the Eocene and Miocene (England and Housemann, 1986; Tapponnier et al., 2001; Wang et al., 2008; Lease et al., 2011, 2012; Craddock et al., 2011; Ding et al., 2022; Peng et al., 2019; Zhao et al., 2023; Chen et al., 2024; Zhang et al., 2020). Low-temperature

https://doi.org/10.5194/egusphere-2024-3191
Preprint. Discussion started: 5 December 2024

thermochronology data, along with thermal history reconstructions constrained by AHe and AFT, reveal rapid uplift during the Eocene to Miocene, likely a result of the far-field effects of the Cenozoic uplift of the northeastern Tibetan Plateau and the northwestward subduction of the Pacific Plate.

Overall, the study area has undergone the Indosinian, Yanshanian, and Himalayan orogenys since the Mesozoic era. The Indosinian tectonic stress originated from the collision and docking of the South China Plate and the North China Plate during the Triassic period, resulting in a north-south stress field. The tectonic stress of the Yanshanian orogeny originated from the Tethys tectonic domain, eastward compression of the Alxa block, westward subduction of the Pacific plate, and closure of the Okhotsk Ocean. In the northern part of the western margin of the basin, the Alxa rigid block sandwiched between the South China and North China plates is squeezed out in a southeast direction, directly affecting the Helanshan Mountains and the northern part of the western margin of the basin, causing the stress direction to shift towards a nearly east-west direction. The direction of the tectonic stress field in the Himalayan orogeny is influenced by the combined action of the Pacific Plate and the Tethys tectonic domain, changing from a north-south direction to a northeast direction. The main source of stress is the Tethys tectonic domain in the southwestern part of the study area.

https://doi.org/10.5194/egusphere-2024-3191
Preprint. Discussion started: 5 December 2024

6 Conclusion

（1）This study utilizes Apatite Fission Track (AFT) and Apatite (U-Th)/He (AHe) dating methods, combined with thermal history modeling and existing geological evidence, to precisely constrain the uplift and cooling history of the central and northern sections of the western Ordos Basin. The analysis reveals significant differences in the timing and intensity of uplift across different regions: Zhuozishan part experienced a large-scale uplift during the Late Jurassic (160-150 Ma), followed by slow uplift between 130-30 Ma, and a more intense uplift phase after 30 Ma; Taole-Hengshanbao part began uplifting around 155-145 Ma, followed by a period of slow uplift between 145-30 Ma, and experienced another phase of rapid uplift after 30 Ma; Majiatan-Huianbao part experienced a significant uplift between 158-137 Ma, with a slower uplift phase from 137-110 Ma, and a period of rapid uplift again between 70-50 Ma. Overall, the northern and southern sections began uplifting earlier, while the middle section initiated uplift slightly later. These findings highlight the spatial variation in uplift timing and rates within the western Ordos Basin.

（2）This study effectively reveals the uplift movements of the northern section of the western margin during the Mesozoic and Cenozoic using low-temperature thermochronology method. It suggests that the Yanshanian orogeny had the most significant tectonic impact on the study

https://doi.org/10.5194/egusphere-2024-3191
Preprint. Discussion started: 5 December 2024

area. Multiple uplift events during the Mesozoic are responses to the multi-phase Yanshanian orogeny in this region. Since the Cenozoic, rapid uplift influenced by the Himalayan orogeny has shaped the current landscape.

Competing interests

The contact author has declared that none of the authors has any competing interests.

Acknowledgements

Financial support for this study were jointly provided by the Major Projects of Changqing Oilfield Company (ZDZX2021). Our heartfelt gratitude is given to those anonymous reviewers for their scientific and linguistic revisions to the manuscript.

Conferences

[1] Bao Hongping, Shao Dongbo, Hao Songli, et al. Basement Structure and Early Sedimentary Cover Evolution of the Ordos Basin[J]. Earth Science Frontiers, 2019, 26(1): 33-43.

[2] Barbarand J, Carter A, Wood I, et al. Compositional and structural control of fission-track annealing in apatite[J]. Chemical Geology, 2003, 198(1-2): 107-137.

[3] Carlson W D, Donelick R A, Ketcham R A. Variability of apatite fission-track annealing kinetics: I. Experimental results[J]. American mineralogist, 1999, 84(9): 1213-1223.

[4] Chen G M, Qin H T, Huang X F, et al. Cenozoic tectonic evolution of the Liupan Shan area: Evidence from zircon and apatite fission tracks[J]. Chinese Journal of Geophysics, 2024, 67(3): 1147-1168.

[5] Chen Gang, Wang Zhiwei, Bai Guojun, Sun Jianbo, Zhang Huiruo, Li Xiangdong. Peak Age Events and Their Sedimentary-Tectonic Responses in the Mesozoic-Cenozoic Ordos Basin[J]. Geology in China, 2007(03): 375-383.

[6] Chen Gang. Composition of Mesozoic Terrigenous Clastic Rocks and Their Tectonic Attributes in the Ordos Basin[J]. Acta Sedimentologica Sinica, 1999(03): 409-413.

[7] Craddock W, Kirby E, Zhang H P. 2011. Late Miocene-Pliocenerange growth in

the interior of the northeastern TibetanPlateau, Lithosphere,3(6):420-438.
[8] Darby B J, Ritts B D. Mesozoic contractional deformation in the middle of the Asian tectonic collage: the intraplate Western Ordos fold–thrust belt, China[J]. Earth and Planetary Science Letters, 2002, 205(1-2): 13-24.
[9] Darby B J, Ritts B D. Mesozoic structural architecture of the Lang Shan, North-Central China: Intraplate contraction, extension, and synorogenic sedimentation[J]. Journal of Structural Geology, 2007, 29(12): 2006-2016.
[10] Ding L, Kapp P, Cai F, et al. Timing and mechanisms of Tibetan Plateau uplift[J]. Nature Reviews Earth & Environment, 2022, 3(10): 652-667.
[11] Dong Shuwen, Zhang Yueqiao, Chen Xuanhua, et al. Formation and Deformation Characteristics of the Late Jurassic Multidirectional Convergent Tectonic System in East Asia[J]. Acta Geoscientia Sinica, 2008, 29(3): 306-317.
[12] Dong Shuwen, Zhang Yueqiao, Li Hailong, et al. The "Yanshan Movement" and the Late Mesozoic Multiplate Convergence Tectonics in East Asia: Commemorating the 90th Anniversary of the "Yanshan Movement"[J]. Science in China: Earth Sciences, 2019, 49(6): 913-938.
[13] Dong Shuwen, Zhang Yueqiao, Long Changxing, et al. New Interpretations of the Jurassic Tectonic Transformations and the Yanshan Movement in China[J]. Acta Geologica Sinica, 2007, 81(11): 1449-1461.
[14] Dong Yunpeng, Li Wei, Zhang Feifei, et al. Formation and Evolution of the Helan Mountain in the Northern Section of the North-South Tectonic Belt[J]. Journal of Northwest University (Natural Science Edition), 2021, 51(6): 951-968
[15] England P, Houseman G, 1986. Finite strain calculations of continentaldeformation:2.Comparison with the India-Asia Collision Zone.Journalof Geophysical Research:Solid Earth,9l(B3):3664-3676.
[16] Farley K A, Wolf R A, Silver L T. The effects of long alpha-stopping distances on (U-Th)/He ages[J]. Geochimica et cosmochimica acta, 1996, 60(21): 4223-4229.
[17] Faure M, Lin W, Chen Y. Is the Jurassic (Yanshanian) intraplate tectonics of North China due to westward indentation of the North China block?[J]. Terra Nova, 2012, 24(6): 456-466.
[18] Flowers R M, Farley K A, Ketcham R A. A reporting protocol for thermochronologic modeling illustrated with data from the Grand Canyon[J]. Earth and Planetary Science Letters, 2015, 432: 425-435.
[19] Gallagher K. Transdimensional inverse thermal history modeling for quantitative thermochronology[J]. Journal of Geophysical Research: Solid Earth, 2012, 117(B2).
[20] Gan Kewen. On the Genesis Mechanism of Thrust Belts and Hydrocarbon Prospects of the Western Margin of the Ordos Basin[J]. In: Yang Junjie. Thrust Tectonics and Hydrocarbon in the Western Ordos Basin. Lanzhou: Gansu Science and Technology Press, 1990, 31239.
[21] Gao Feng, Wang Yuejun, Liu Shunsheng, Hu Baoqing. Study on the Thermal History of the Western Margin of the Ordos Basin Using Apatite Fission Track Analysis[J]. Geotectonica et Metallogenia, 2000(01): 87-91.
[22] Gao Shaohua. Mesozoic-Cenozoic Evolutionary Modification of the Lateral Structural Belt in the Central Western Ordos Basin and Its Significance for Oil and

https://doi.org/10.5194/egusphere-2024-3191
Preprint. Discussion started: 5 December 2024

Gas[D]. Xi'an: Northwest University, 2014.

[23] Gleadow A J W, Seiler C, Rink W J, et al. Fission track dating and thermochronology[J]. Encyclopedia of scientific dating Methods, 2015: 285-296.

[24] Hasebe N, Barbarand J, Jarvis K, et al. Apatite fission-track chronometry using laser ablation ICP-MS[J]. Chemical Geology, 2004, 207(3-4): 135-145.

[25] He Dengfa, Sun Fangyuan, Zhai Yonghe, et al. Formation Evolution of the Shigouyi Anticline in the Western Ordos Basin and Its Tight Sandstone Gas Accumulation Model[J]. Oil & Gas Geology, 2021, 42(2): 370-390.

[26] Jiang Suyang, Huang Wenhui, Zhang Yongsheng, et al. Tectonic Setting and Provenance Analysis of the Sandstones from the Sandaokan Formation in the Northern Segment of the Western Ordos Basin[J]. Journal of Northeast Petroleum University, 2019, 43(4): 17-28.

[27] Ketcham R A, Carter A, Donelick R A, et al. Improved modeling of fission-track annealing in apatite[J]. American Mineralogist, 2007, 92(5-6): 799-810.

[28] Ketcham R A. Forward and inverse modeling of low-temperature thermochronometry data[J]. Reviews in mineralogy and geochemistry, 2005, 58(1): 275-314.

[29] Lease R O,Burbank D W, Hough B, et al. 2012. Pulsed Miocenerange growth in northeastern Tibet: insights from XunhuaBasin magnetostratigraphy and provenance. GSA Bull.,124(5-6):657-677.

[30] Lease R.O., Burbank D W, Clark M K, et al. 2011. Middle Miocenereorganization of deformation along the northeastern TibetanPlateau, Geology,39(4):359-362.

[31] Lei Q, Yu J, Zhang P, et al. Tectonic geomorphology and prehistoric earthquakes of the West Helanshan fault, West Ordos, and its implications for regional tectonics and seismic hazard[J]. Tectonophysics, 2022, 833: 229375.

[32] Li Bin. Study on the Thrust Belt Structure and Hydrocarbon Controlling Factors in the Western Ordos Basin[D]. Northwest University, 2019.

[33] Li Bin. Tectonic Characteristics and Hydrocarbon Accumulation Studies of the Foreland Basin in the Western Ordos Basin[D]. Graduate School of the Chinese Academy of Sciences (Guangzhou Institute of Geochemistry), 2006.

[34] Li Tianbin. Characteristics and Evolution of Thrust Structures in the Western Ordos Basin[D]. China University of Geosciences (Beijing), 2006.

[35] Liu Chiyang, Zhao Hongge, Wang Feng, et al. Mesozoic Tectonic Characteristics of the Western Margin of the Ordos Basin[J]. Acta Geologica Sinica, 2005, 79(6): 737-747.

[36] Liu Hefu. Types of Foreland Basins and Styles of Fold-Thrust Structures[J]. Earth Science Frontiers, 1995, 2(3): 59-68.

[37] Liu Jianhui. Cenozoic Extensional Uplift of the Helan Mountains and Qinling Mountains and Analysis of Fault Frictional Heating Using Apatite Fission Track Method[J]. International Seismological Dynamics, 2010, 31(3): 31-33.

[38] Liu S F, The coupling mechanism of basin and orogen in the western ordos Basin and adjacent regionsof China[]. Journal of Asian Eart h Science,1998,16(4):369-383.

[39] Liu Shaofeng, Yang Shigong. North-South Differences and Their Formation Mechanism on the Western Margin of the Ordos Basin[J]. Geological Science, 1997, 32(3): 397-408.
[40] Ma Jinghui, He Dengfa. Mesozoic-Cenozoic Tectonic Events in the Helan Mountain Tectonic Belt and Adjacent Areas: Constraints from Unconformities and Fission Track Analysis[J]. Acta Petrologica Sinica, 2019, 35(4): 1121-1142.
[41] Ma X.H., Xing L.S., Yang Z.Y., et al. Paleomagnetic Study of the Ordos Basin since the Late Paleozoic [J]. Chinese Journal of Geophysics, 1993, (01): 68-79.
[42] Ouyang Zhengjian, Chen Hongde, Feng Juanping. Tectonic Characteristics and Evolution of the Central and Southern Segments of the Western Margin of the Ordos Basin[J]. Modern Geology, 2012, 26(04): 691-695.
[43] Peng H , Wang J , Liu C ,et al.Thermochronological constraints on the Meso-Cenozoic tectonic evolution of the Haiyuan-Liupanshan region, northeastern Tibetan Plateau[J].Journal of Asian earth sciences, 2019, 183(Oct.1):103966.1-103966.13.
[44] Peng H, Wang J, Liu C, et al. Mesozoic exhumation and ca. 10 Ma reactivation of the southern Yin Shan, North China, revealed by low-temperature thermochronology[J]. Tectonophysics, 2022, 823: 229189.
[45] Peng Heng. Fission Track Thermochronology Analysis and Its Geological Significance in the Southwestern Adjacent Area of the Ordos Block[D]. Northwest University, 2020.
[46] Rao G, Chen P, Hu J, et al. Timing of Holocene paleo-earthquakes along the Langshan Piedmont Fault in the western Hetao Graben, North China: Implications for seismic risk[J]. Tectonophysics, 2016, 677: 115-124.
[47] Ren Zhanli, Cui Junping, Qi Kai. New Advances in the Theoretical Research and Methods for Restoring the Thermal Evolution History of Deep and Ultra-deep Layers in Overlapping Basins[J]. Journal of Northwest University (Natural Science Edition), 2022, 52(6): 910-929.
[48] Ren Zhanli, Liu Li, Cui Junping, et al. Application of Tectonic Thermal Evolution History in the Study of Hydrocarbon Accumulation Phases[J]. Oil & Gas Geology, 2008, 29(4): 502-506.
[49] Ren Zhanli, Qi Kai, Liu Runchuan, et al. The Dynamical Background of Early Cretaceous Tectonic Thermal Events in the Ordos Basin and Their Control on the Accumulation Periods of Various Minerals, Including Oil and Gas[J]. Acta Petrologica Sinica, 2020, 36(4): 1213-1234.
[50] Ren Zhanli, Tian Tao, Li Jinbu, et al. Research Methods for Thermal Evolution History of Sedimentary Basins and Progress in Reconstructing Thermal Evolution History of Overlapping Basins[J]. Journal of Earth Sciences and Environment, 2014, 36(3): 1-20.
[51] Ren Zhanli, Yu Qiang, Cui Junping, Qi Kai, Chen Zhanjun, Cao Zhanpeng, Yang Peng. Thermal Evolution History of the Ordos Basin and Its Control on Hydrocarbons[J]. Earth Science Frontiers, 2017, 24(03): 137-148.
[52] Ren Zhanli, Zhang Sheng, Gao Shengli, Cui Junping, Xiao Yuanyuan, Xiao Hui. Tectonic Thermal Evolution History of the Ordos Basin and Its Significance for

Accumulation and Mineralization[J]. Science in China: Series D, Earth Sciences, 2007(S1): 23-32.

[53] Ren Zhanli. Study on the Geothermal History of the Ordos Basin Using the Apatite Fission Track Method[J]. Chinese Journal of Geophysics, 1995, 38(03): 339-349..

[54] Tang Xiyuan, Guo Zhongming, Wang Dingyi. Characteristics, Evolution, and Hydrocarbon Exploration of the Thrust Nappe Structure Belt in the Western Ordos Basin[J]. Oil & Gas Geology, 1988, 9(1): 1-10.

[55] Tang Xiyuan. Thrust Nappe Structures and Hydrocarbon Exploration on the Western Margin of the Shaanxi-Gansu-Ningxia Basin[M]. Xi'an: Northwest University Press, 1992.

[56] Tapponnier P, XuZ Q, Roger F, et al. 2001. Oblique stepwise riseand growth of the Tibet Plateau. Science, 294(5547):1671-1677.

[57] Tian Chaoyang, Chen Hong, Liu Xinshe, et al. Fission Track Ages and Mesozoic Tectonic Uplift in the Niushou Mountain—Luoshan Area of the Western Ordos[J]. Journal of Geological Mechanics, 2023, 29(05): 599-617.

[58] Vermeesch P. RadialPlotter: A Java application for fission track, luminescence and other radial plots[J]. Radiation Measurements, 2009, 44(4): 409-410.

[59] Wang CS, Zhao XX,Liu ZF, et al.2008. Constraints on the earlyuplift history of the Tibetan Plateau, Proc, Natl. Acad. Sci.USA，105(13):4987-4992

[60] Yang Hua, Fu Jinhua, Ouyang Zhengjian, Sun Liuyi. Analysis of Tectonic-Sedimentary Environments during the Late Triassic in the Western Margin of the Ordos Basin[J]. Acta Sedimentologica Sinica, 2011, 29(03): 427-439.

[61] Yang J.J., Zhang B.R. Basic Characteristics of the Overthrust Belt on the Western Margin of the Ordos Basin[A]. In: Yang J.J., Zhao Z.Y., Liu H.F., et al. Structure and Oil and Gas of the Overthrust Belt on the Western Margin of the Ordos Basin[C]. Lanzhou: Gansu Science and Technology Press, 1990. 91-105.

[62] Yang Junjie, Zhang Borong. Strike-Slip Rift and Associated Thrust Belt: A Case Study of the Yinchuan Graben and Hengshanpu Thrust Belt[J]. Petroleum Exploration and Development, 1986(02): 1-8.

[63] Yang S.B., Geng X.X., Guo Q.Y., et al. Mesozoic Tectonic Evolution in the Northern Section of the Western Margin of the Ordos Basin[J]. Geological Review, 2008, 54(3): 307-315.

[64] Yang Shengbin, Geng Xinxia, Guo Qingyin, et al. Mesozoic Tectonic Evolution of the Northern Segment of the Western Ordos Basin[J]. Geological Review, 2008, 54(3): 307-315.

[65] Yang Shengbin, Guo Qingyin, Hou Guiting, et al. Subsidence History and Sedimentary Response in the Northern Segment of the Western Ordos Basin[J]. Journal of Peking University: Natural Science Edition, 2006, 42(2): 192-198.

[66] Zhai Mingguo. The Formation, Evolution, and Metallogenesis of the North China Craton[J]. Mineral Deposits, 2010 (1): 24-36.

[67] Zhai Mingguo. The Ordos Block: The Key to Unraveling the Mysteries of Early Continental Formation, Evolution, and Tectonic Regime of the North China Craton[J]. Chinese Science Bulletin, 2021, 66(26): 3441-3461.

[68] Zhang Chengli, Gou Longlong, Liu Xinyu, et al. Precambrian Geological Events, Nature, and Geological Significance of the Basement in the Western North China Craton[J]. Acta Petrologica Sinica, 2018, 34(4): 981-998.

[69] Zhang Guowei, Dong Yunpeng, Yao Anping. A New Starting Point for the Study of Orogenic Belts and Orogenesis[J]. Northwest Geology, 2001, 34(1): 1-9.

[70] Zhang J, Cunningham D, Qu J, et al. Poly-phase structural evolution of the northeastern Alxa Block, China: Constraining the Paleozoic-Recent history of the southern central Asian Orogenic belt[J]. Gondwana Research, 2022, 105: 25-50.

[71] Zhang J, Wang Y, Qu J, et al. Mesozoic intracontinental deformation of the Alxa Block in the middle part of Central Asian Orogenic Belt: A review[J]. International Geology Review, 2021, 63(12): 1490-1520.

[72] Zhang J, Yun L, Zhang B, et al. Deformation at the easternmost Altyn Tagh Fault: Constraints on the growth of the northern Qinghai–Tibetan plateau[J]. Acta Geologica Sinica-English Edition, 2020, 94(4): 988-1006.

[73] Zhang J., Ma Z.J., Ren W.J. Mechanism of North-South Differences in the Overthrust Belt on the Western Margin of the Ordos Basin[J]. Geotectonica et Metallogenia, 2000(02): 124-133.

[74] Zhang Jiasheng, He Zixin, Fei Anqi, et al. Large Margin Thrust Nappe System in the Northern Segment of the Western Ordos Basin[J]. Geological Science, 2008, 43(2): 251-281.

[75] Zhang Jin, Zhang Beihang, Zhao Heng, et al. Characteristics and Mechanisms of Late Cenozoic Deformation in the Beishan-Alashan Region[J]. Earth Science Frontiers, 2023, 30(5): 334.

[76] Zhao Chongyuan, Liu Chiyang, Ren Zhanli. Geology of Oil and Gas Basins and System Engineering in Their Research[J]. Oil & Gas Geology, 1990, 11(1): 108-113.

[77] Zhao D., Chen P., Li R.X., et al. Basin Records of Multistage Tectonic Uplift in the Longshou Mountain of the Northeastern Tibetan Plateau during the Late Cenozoic [J]. Acta Petrologica Sinica, 2023, 39(12): 3759-3774.

[78] Zhao Hongge, Liu Chiyang, Wang Feng, et al. Tectonic Partitioning and Characteristics of the Western Margin of the Ordos Basin[J]. Oil & Gas Geology, 2006, 27(2): 173-179.

[79] Zhao Hongge, Liu Chiyang, Wang Feng, et al. Uplift Timing and Evolution of the Helan Mountains[J]. Science in China: Series D, 2007, 37(A01): 185-192.

[80] Zhao Hongge, Liu Chiyang, Wang Jianqiang, et al. Exploration of Tectonic Attributes during the Late Triassic in the Western Ordos Basin[J]. Geological Journal of China, 2007, 34(3): 384-391.

[81] Zhao Hongge, Liu Chiyang, Yao Yaming, Wang Feng, Yin Yan. Fission Track Evidence of Differential Uplift in the Western Ordos Basin[J]. Journal of Northwest University (Natural Science Edition), 2007, (03): 470-474.

[82] Zhao Hongge. Tectonic Characteristics and Evolution of the Western Ordos Basin[D]. Northwest University, 2003.

[83] Zhao Pan, Xu Bei, Chen Yan. Mongolian–Okhotsk Ocean: Evolutionary Process and Final Closure[J]. Science in China: Earth Sciences, 2023, 53(11): 2541-2559.

[84] Zhao X, Coe R S. 1987.Palaeomagnetic constraints on the collision and rotation

https://doi.org/10.5194/egusphere-2024-3191
Preprint. Discussion started: 5 December 2024

of North and SouthChina. Nature, 327:41-144.

[85] Zhao Xiaochen. Mesozoic Tectonic Evolution and Later Modification of the Northern Section of the North-South Tectonic Belt in China[D]. Xi'an: Northwest University, 2017.

[86] Zhao Y, Liu X, Hu J, et al. Metamorphism of diverse basement gneisses of the Ordos Basin: Record of multistage Paleoproterozoic orogenesis and constraints on the evolution of the western North China Craton[J]. Precambrian Research, 2019, 328: 48-63.

[87] Zhuo Yuzhou. Determination of Mesozoic-Cenozoic Uplift Events in the Zhuozishan Area of the Northwestern Ordos Basin and Their Tectonic Significance[D]. Northwest University, 2015.